Check for updates

Received: 10 December 2018 | Accepted: 3 February 2021

DOI: 10.1002/stem.3358

EMBRYONIC STEM CELLS/INDUCED PLURIPOTENT STEM CELLS

STEM CELLS

A synthetic mRNA cell reprogramming method using *CYCLIN D1* promotes DNA repair, generating improved genetically stable human induced pluripotent stem cells

Ana Belén Alvarez-Palomo[1,2] | Jordi Requena-Osete[1,3,4] | Raul Delgado-Morales[5,6] | Victoria Moreno-Manzano[7] | Carme Grau-Bove[1] | Agueda M. Tejera[8] | Manel Juan Otero[9] | Carme Barrot[10] | Irene Santos-Barriopedro[5] | Alejandro Vaquero[5] | Jovita Mezquita-Pla[1,11] | Sebastian Moran[5] | Carlos Hobeich Naya[12,13] | Iris Garcia-Martínez[12,13] | Francisco Vidal Pérez[12,13,14] | María A. Blasco[8] | Manel Esteller[15,16,17,18] | Michael J. Edel[1,19,20,21]

[1]Molecular Genetics and Control of Pluripotency Laboratory, Department of Biomedicine, Institute of Neuroscience, Faculty of Medicine, University of Barcelona, Hospital Clinic, Barcelona, Catalonia, Spain

[2]Cell Therapy Service, Banc de Sang i Teixits (BST), Barcelona, Spain

[3]Institute of Clinical Medicine, University of Oslo, Oslo, Norway

[4]Division of Mental Health and Addiction, NORMENT, Centre for Mental Disorders Research, Oslo, Norway

[5]Chromatin Biology Laboratory, Cancer Epigenetics and Biology Program (PEBC), Bellvitge Biomedical Research Institute (IDIBELL), L'Hospitalet de Llobregat, Barcelona, Catalonia, Spain

[6]Department of Psychiatry and Neuropsychology, School for Mental Health and Neuroscience (MHeNs), Maastricht University, Maastricht, The Netherlands

[7]Neuronal and Tissue Regeneration Laboratory, Príncipe Felipe Research Center, Valencia, Spain

[8]Telomeres and Telomerase Group, Molecular Oncology Program, Spanish National Cancer Centre (CNIO), Madrid, Spain

[9]Hospital Clinic, Department of Clinical Immunology, Biomedical Diagnostic Center (CDB), Villarroel, Catalonia, Spain

[10]Forensic Genetics Laboratory, Legal Medicine Department, Faculty of Medicine, University of Barcelona, Barcelona, Spain

[11]Institut d'Investigacions Biomèdiques August Pi i Sunyer (IDIBAPS), Barcelona, Catalonia, Spain

[12]Congenital Coagulopathies Department, Banc de Sang i Teixits (BST), Barcelona, Spain

[13]Transfusional Medicine, Vall d'Hebron Research Institute, Universitat Autònoma de Barcelona (VHIR-UAB), Barcelona, Spain

[14]CIBER de Enfermedades Cardiovasculares (CIBERCV), Madrid, Spain

[15]Josep Carreras Leukemia Research Institute (IJC), Badalona, Barcelona, Catalonia, Spain

[16]Centro de Investigacion Biomedica en Red Cancer (CIBERONC), Madrid, Spain

[17]Institucio Catalana de Recerca i Estudis Avançats (ICREA), Barcelona, Catalonia, Spain

[18]Physiological Sciences Department, School of Medicine and Health Sciences, University of Barcelona (UB), Barcelona, Catalonia, Spain

[19]Victor Chang Cardiac Research Institute, Sydney, New South Wales, Australia

[20]University of Western Australia, School of Medicine and Pharmacology, Harry Perkins Research Institute, Centre for Cell Therapy and Regenerative Medicine (CCTRM), Perth, Western Australia, Australia

[21]Centro de Oftalmología Barraquer, Institut Universitari Barraquer, Universitat Autònoma de Barcelona, Bellaterra, Spain

Ana Belén Alvarez-Palomo and Jordi Requena-Osete contributed equally to this study.

[Correction added on 6 March 2021, after first online publication: Affiliation for the author Jovita Mezquita-Pla has been modified.]

This is an open access article under the terms of the Creative Commons Attribution-NonCommercial-NoDerivs License, which permits use and distribution in any medium, provided the original work is properly cited, the use is non-commercial and no modifications or adaptations are made.
© 2021 The Authors. STEM CELLS published by Wiley Periodicals LLC on behalf of AlphaMed Press.

Correspondence
Michael J. Edel, PhD, Centro de Oftalmología Barraquer, Institut Universitari Barraquer, Bellaterra, Spain.
Email: michaeledel@barraquer.com, edel.michael@gmail.com

Funding information
Consejo Superior de Investigaciones Científicas, Grant/Award Numbers: RYC-2010-06512, BFU2011-26596, BFU2014-54467-P; TV3 Marato project, Grant/Award Number: FBG309768; European Commission; Generalitat de Catalunya; EU; Worldwide Cancer Research; Banco Santander; Fundación Botín; European Regional Development Fund; Spanish Ministry of Science and Innovation; Fondo Europeo de Desarrollo Regional; Fundació La Marató de TV3; Agencia Estatal de Investigación; Ministerio de Ciencia e Innovación; FEDER; Fundació La Marató de TV3; University of Barcelona

Abstract

A key challenge for clinical application of induced pluripotent stem cells (iPSC) to accurately model and treat human pathologies depends on developing a method to generate genetically stable cells to reduce long-term risks of cell transplant therapy. Here, we hypothesized that *CYCLIN D1* repairs DNA by highly efficient homologous recombination (HR) during reprogramming to iPSC that reduces genetic instability and threat of neoplastic growth. We adopted a synthetic mRNA transfection method using clinically compatible conditions with *CYCLIN D1* plus base factors (*OCT3/4*, *SOX2*, *KLF4*, *LIN28)* and compared with methods that use *C-MYC*. We demonstrate that *CYCLIN D1* made iPSC have (a) lower multitelomeric signal, (b) reduced double-strand DNA breaks, (c) correct nuclear localization of RAD51 protein expression, and (d) reduced single-nucleotide polymorphism (SNP) changes per chromosome, compared with the classical reprogramming method using *C-MYC*. *CYCLIN D1* iPSC have reduced teratoma Ki67 cell growth kinetics and derived neural stem cells successfully engraft in a hostile spinal cord injury (SCI) microenvironment with efficient survival, differentiation. We demonstrate that *CYCLIN D1* promotes double-stranded DNA damage repair predominantly through HR during cell reprogramming to efficiently produce iPSC. *CYCLIN D1* reduces general cell stress associated with significantly lower *SIRT1* gene expression and can rescue *Sirt1* null mouse cell reprogramming. In conclusion, we show synthetic mRNA transfection of *CYCLIN D1* repairs DNA during reprogramming resulting in significantly improved genetically stable footprint in human iPSC, enabling a new cell reprogramming method for more accurate and reliable generation of human iPSC for disease modeling and future clinical applications.

KEYWORDS
cellular therapy, induced pluripotent stem cells, neural stem cells (NSCs), cell cycle, clinical translation

1 | INTRODUCTION

Human induced pluripotent stem cells (iPSC) have immense clinical potential as a source of patient matched immunologically compatible cells for cell replacement therapies and disease modeling and thus are studied intensely. Human iPSC can be generated from adult somatic cells reprogrammed by ectopic expression defined transcription factors (*OCT3/4*, *SOX2*, *KLF4*, *C-MYC*) with similar characteristics to embryonic stem cells (ESC), albeit iPSC have a higher tumorigenic potential than ESC[1-3] . The RIKEN clinical trial to treat macular degeneration uses retinal pigmented epithelial cells derived from iPSC generated by episomal methods and includes the use of *C-MYC*.[4,5] This trial identified a number of genomic alterations resulting in removal of the patient from the clinical trial. These stringent guidelines take into consideration the long-term effects of transplanted iPSC-derived cells, essential for its long-term success. This creates a pressing need to define a standard operating procedure (SOP) to reduce global genetic instability and more reliably generate human iPSC for clinically compatible applications.[4,5]

Current methodologies to generate human iPSC can be broadly categorized based on the mode of ectopic gene delivery: viral[2,6-9] or nonviral.[10-15] One nonviral route, synthetic mRNA transfection, has a number

Significance statement

A key challenge for clinical application of induced pluripotent stem cells (iPSC) to accurately model and treat human pathologies lies in developing a method for their generation that is genetically stable to reduce long-term risks of cell transplant therapy. The authors report that synthetic mRNA transfection of *CYCLIN D1* repairs DNA during reprogramming, resulting in significantly improved genetically stable footprint in human iPSC, enabling more accurate and reliable generation of human iPSC for disease modeling and future clinical applications.

of advantages over traditional viral approaches: it is fast acting, allows fine titration of gene dosage, generates less aneuploidy, and mRNA particles degrade after 48 hours with no genetic insertion or DNA scarring.[12,13,16]

It is well established that canonical cell reprogramming methods that use *C-MYC* cause cell replication stress and DNA damage that result in chromosome abnormalities, genomic instability, and iPSC-derived cancers, thus complicating clinical applications.[17-22] Indeed, in another previous study, we found that neural stem cells (NSC) derived from *C-MYC* viral-mediated reprogrammed cells generated neoplastic growth when engrafted to a rat SCI model.[23] Studies of *C-MYC* in iPSC with global chromatin immunoprecipitation (ChIP) array reveal that *C-MYC* regulates many cellular function pathways including promoting the expression of cancer genes.[24-27] Replacing *C-MYC* while maintaining reprogramming efficiency has been analyzed previously, albeit using viral methods or cell types that would have limited clinical application.[7,20,28] Despite advances, the use of *C-MYC* is still currently used in human iPSC in clinical trials, needed to maintain sufficient efficiency to reprogram patient fibroblast cells and prevent spontaneous differentiation of iPSC.[29,30]

In a previous study investigating the role of *REM2* GTPase in human pluripotency, we observed that *CYCLIN D1* could potentially be used in lieu of *C-MYC* in retroviral reprogramming methods of human fibroblasts to an SSEA4+ve "iPSC-like" phenotype; however, these cells were not fully characterized.[4] In normal and cancer cells, *CYCLIN D1* plays a major role in DNA damage repair and its noncanonical functions in DNA repair have been reviewed elsewhere.[31-33] Briefly, *CYCLIN D1* acts in the homologous recombination (HR) pathway by binding BRCA2, helping it to recruit RAD51 monomers to repair double-strand DNA breaks (DSB).[31,34] Contrary to this, *C-MYC* potentiates the "alternative" nonhomologous end joining (NHEJ), by inhibiting miR150/miR22 and *BIN1* (inhibitors of *LIGASE 3* and *PARP*, respectively, both required for alternative NHEJ). This pathway is error prone and leads to higher risk of genetic instability.[35-38] Moreover, *C-MYC* (all MYC family genes including L-MYC) inhibits the "classical" NHEJ by direct interaction with Ku70 through its MYC box II (MBII) domain, subsequently inhibiting DNA-PKC activity essential for DNA repair.[39]

The use of *C-MYC* (and family members) for cell reprogramming is likely to prevent the use of human iPSC-derived cells for future clinical applications, given the risk of genetic mutations. Here, we investigate the potential of using *CYCLIN D1* with the other factors (*OCT3/4*, *SOX2*, *KLF4*, *LIN28*; termed base factors) to generate hiPSC in clinically compatible conditions for future clinical applications. Importantly, we advance our previous work and hypothesize that the use of *CYCLIN D1* will promote DNA damage repair and reduce cell stress during cell reprogramming to improve genetic stability of iPSC. We found that *CYCLIN D1* maintains cell reprogramming efficiency while reducing *SIRT1* gene expression (a marker of general cell stress) repairing DNA damage and DSB by HR during cell reprogramming and results in improved genomic stability of iPSC when compared with canonical methods currently in use for clinical trials.

2 | RESULTS

2.1 | *CYCLIN D1* reprogramming of human skin fibroblasts

We sought a clinically compatible methodology and chose to adopt a synthetic mRNA approach (*OCT3/4*, *SOX2*, *KLF4*, *LIN28*; termed base factors), plus *CYCLIN D1* using feeder free defined cell culture mediums to express the reprogramming factors. The use of synthetic mRNA transfection methods is an efficient and robust method in which mRNA is degraded over 48 hours with no random transgene insertion, no use of virus, low aneuploidy, and no genetic scarring, making it the preferred method for clinical applications.[10,11,14] We chose to utilize human foreskin fibroblasts (HFF), as fibroblasts are easier to obtain from patients in clinically relevant numbers than other specialized cell types, such as cord blood cells.

HFF were transfected with mRNAs of the four base factors (*OCT3/4*, *SOX2*, *KLF4*, *LIN28*; 4F) alone or in combination with *CYCLIN D1* or *C-MYC*. A total of 12 iPSC clones were manually picked from the *C-MYC* condition (MH hiPSC) and 8 iPSC clones from the *CYCLIN D1* condition (DH hiPSC), and after preliminary characterization of MH1-12 and DH1-8 clones, three clones from each condition (*C-MYC*: MH1, MH6, and MH9 hiPSC clones; and *CYCLIN D1*: DH1, DH3, and DH5 hiPSC clones) were fully characterized and compared with commercially available iPSC (generated from younger stable cord blood stem cells with episomal DNA) (Figures 1A and S1A-D). In addition to being positive for ESC marker SSEA4, these cells possessed other markers of fully reprogrammed cells such as expression of endogenous OCT3/4 and SOX2 as well as ESC markers TRA-1-81 and alkaline phosphatase (AP) (Figures 1A and S1B,C). Interestingly, assessment of early reprogramming events (10-14 days) of TRA1-81 expression by flow cytometry demonstrates a low level in 4F alone and a higher percentage of pluripotent cells being formed with *CYCLIN D1* (5.6%) compared with *C-MYC* (1.3%) forming iPSC (Figure S1D). We confirm that *CYCLIN D1* can induce reprogramming in the presence of the canonical four factors minus *C-MYC* using retroviral methods or synthetic mRNA transfection methods with sufficient efficiency to pick numerous colonies and the synthetic mRNA transfection method is more efficient than the retroviral method (Figures 1A, S1A-D, and S2A). We found that transfection of 50 ng of *CYCLIN D1* synthetic mRNA was optimal and higher concentrations did not promote the cell cycle (Figure S2B). Reprogramming efficiency based on AP staining was found to be 0.107% with *CYCLIN D1* and 0.293% for *C-MYC* conditions (Figure S1D). *CYCLIN D1* gene expression was found to be equal in all hiPSC clones generated at passage 10 (Figure S2C). All hiPSC clones expressed markers of pluripotency equivalent to commercially made episomal hiPSC and were positive for AP staining (Figures 1A, S1A, and S2A). We were unable to reprogram HFF using 4F alone to sufficient numbers or quality to expand. All hiPSC clones maintained good cell morphology, proliferated at the same rate passaged every 4 to 5 days and no reversal of cell phenotype was detected over long-term passaging.

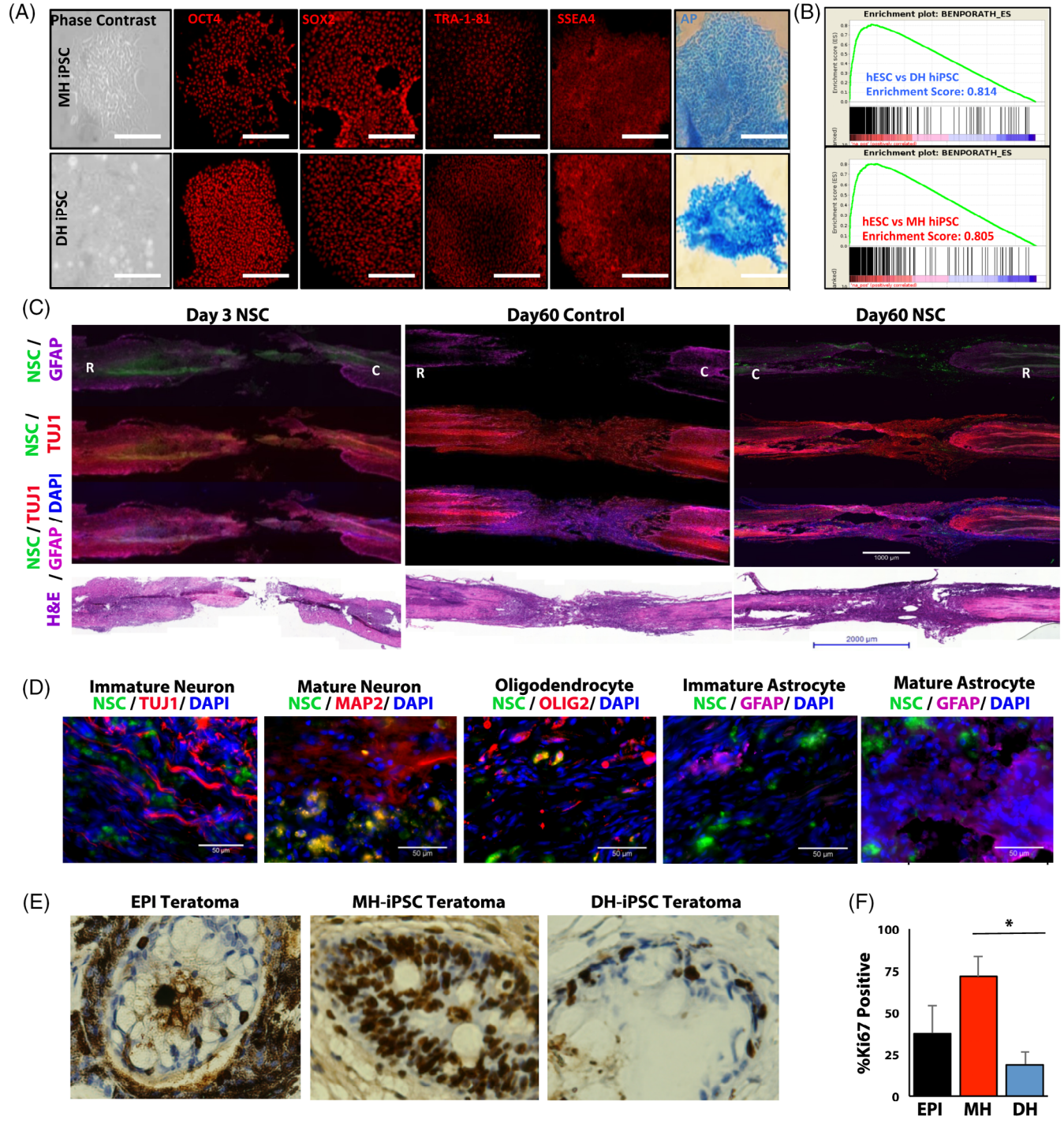

FIGURE 1 *CYCLIN D1* reprograms human cells to induced pluripotent stem cells (iPSC). A, Human iPSC were generated using a modified synthetic mRNA transfection method and a feeder free defined medium cell culture system. One representative clone is shown for every condition. Phase contrast, immunofluorescence for pluripotency markers (in red: *OCT4*, *SOX2*, *TRA1-81*, *SSEA4*), alkaline phosphatase (AP). B, Gene set enrichment analysis (GSEA) of microarray expression profiles comparing the gene profile of *C-MYC* (MH) (bottom) or *CYCLIN D1* (DH) (top) made human iPSC with human embryonic stem cells (hESC). C, Immunofluorescence of perfused spinal cords at 3 and 60 days after transplantation of DH-iPSC derived neural stem cells (NSC). Injected cells were tagged with cell tracker (Green Vybrant CFDA SE). Tuj1 and GFAP were used to detect neurons and astrocytes respectively and 4′,6-diamidino-2-phenylindole (DAPI) to stain nuclei. Merged image shown. *Note*: Green Vybrant cell tracker-positive cells in day 60 NSC transplanted spinal cords. No neoplastic growth was observed with detailed assessment of hematoxylin and eosin (H&E) sections. D, Colocalization study of green cell tracker with different antibodies by immunofluorescence for markers of mature neurons (MAP2), immature neurons (Tuj1), oligodendrocytes (OLIG2), immature astrocytes (GFAP), and mature astrocytes (S100). Sample numbers: n = 4 for control SCI and NSC transplanted spinal cord injury (SCI) rats. E, Teratoma assay of iPSC using commercially available episomal made iPSC as a control cells injected in nude mice and stained for ki67. F, Quantification of ki67 staining (n = 3) (*$P \leq .05$)

Further characterization by microarray gene set enrichment analysis (GSEA) shows that upregulated genes in MH and DH hiPSC are both highly significantly enriched in human ESC signature (ES1 and ES2 combined) (Figure 1B). We next assessed their functionality with in vitro differentiation by general and guided differentiation to the three germ layers, to NSC, to definitive endoderm (DE), and cardiomyocytes (CM) and demonstrated the presence of tissue specific markers for all three germ layers and cell types by immunofluorescence, flow cytometry and reverse transcription polymerase chain reaction (RT-PCR) (Figures S3A-E and S4).

We next sought to assess the ability of DH-iPSC to engraft and survive in vivo when transplanted in a model of cell replacement therapy (outlined in Figure S5A). To this end, we first differentiated DH-iPSC to a NSC fate and found DH-iPSC made NSC at similar efficiency to MH-iPSC and commercial human iPSC made from episomal methods by Nestin and Tuj1 immunofluorescence (Figures S3C and S4B). We next transplanted clinically compatible DH-iPSC-derived NSC into the spinal cord of injured rats and demonstrated engraftment and survival in the hostile tissue niche at day 3 and at 2 months with no neoplastic growth observed in the spinal cords (Figures 1C,D and S5B,C). Detailed assessment of hematoxylin and eosin (H&E)-stained sections of the spinal cords could not detect any evidence of proliferative growth (Figure 1C, bottom panel). DH-iPSC-derived NSC successfully differentiated into mature neurons (75.1% MAP2 positive), oligodendrocytes (18.2% Olig2), and mature astrocytes (5.2% S-100) with a low percentage of immature neurons (1.9% TUJ1) (Figure 1D).

We have previously shown that c-Myc-made iPSC-derived NSC, using retroviral methods, are transplanted in the rat SCI model results in neoplastic growth with approximately 5% Ki67-positive NSC 2 months after transplantation.[23] Although using a different method, we did not observe any neoplastic growth from DH-iPSC-NSC cells made by synthetic mRNA methods in the SCI transplant model with 0.07% Ki67-positive transplanted cells 2 months after transplantation, suggesting that synthetic mRNA made DH-iPSC-NSC have significantly less risk of neoplastic growth than MH-iPSC (Figure S5D). To test whether *CYCLIN D1* reprogrammed cells are in fact less neoplastic than *C-MYC* synthetic mRNA transfected made reprogrammed cells we performed a teratoma assay. Assessment of teratomas by H&E staining revealed that all hiPSC clones could differentiate properly into the three germs layers in vivo and that DH teratomas had a slower growth rate than MH teratomas, similar to commercially available episomal made teratomas that are derived from younger cord blood stem cells (Figures 1E,F and S6A-D). Assessment of Ki67 expression demonstrated that DH teratomas have a significantly reduced level of cell proliferation in all three germ layers compared with MH hiPSC, and lower levels than episomal made iPSC teratoma (Figure 1F). This demonstrates that *CYCLIN D1* made human iPSC can significantly reduce the risk of neoplastic growth.

2.2 | DH-iPSC have greater genomic stability than iPSC reprogrammed with classical method

We hypothesized that given *CYCLIN D1*'s well-known role in DNA damage repair in normal cells, the use of *CYCLIN D1* would result in increased genomic stability in human iPSC. Therefore, we sought to determine the quality of the resulting iPSC cells by investigating several hallmarks of genomic stability. We found that DH-iPSC had significantly fewer DSB as measured by H2AX staining than MH-iPSC and that this persisted when cells were differentiated to NSC (Figure 2A,B). Assessment of karyotype found no differences between human iPSC clones from either method and all were normal karyotype (Figure S7A). Using fluorescence in situ hybridization (FISH) for telomere length analysis, we found a significantly reduced percentage of multitelomeric signal (MTS) "footprint" in DH iPSC (passage 10) and derived iNSC compared with MH iPSC (Figures 2C and S7B). The increase in MTS signal observed in MH hiPSC is indicative of increased telomere fragility associated with genetic instability, degenerative pathologies, and cancer.[40] Using an infinium Omni 5-4V1.2 array-based approach we found that DH-iPSC had reductions in both differences in global SNP and copy number variation (CNV); however, these were not statistically significant from the starting HFF cells (Figure 2D,E). Analyzing the SNP array data in more depth for SNP changes per chromosome (0, 1, or 2 changes), we found that DH-iPSC had less SNP changes than MH-iPSC per chromosome, suggesting better genetic stability in DH-iPSC (Figure 2F,G). Annotating further the SNP changes in the genetic regions we observed that *CYCLIN D1*-generated hiPSC have less SNPs in different noncoding genetic regions (inner circle—842 SNPs in total) compared with the classical method currently in use for clinical applications using *C-MYC*-generated hiPSC (outer circle—2569 SNPs in total) (Figure 2H). Furthermore, *CYCLIN D1*-generated hiPSC had less cancer-related genes with SNPs (Figure 2I). These data demonstrate that *CYCLIN D1*-generated hiPSC have significantly improved genomic stability than current clinical grade methods that use *C-MYC*, and thus clinically advantageous to reduce risk for long-term cell replacement transplant strategies or accurate disease modeling.

2.3 | *CYCLIN D1* preferentially repairs DSB by the more efficient HR

It is well established in normal somatic cells that *CYCLIN D1* repairs DSB via the HR pathway[31,34] while *C-MYC* potentiates the "alternative" nonhomologous end joining (Alt. NHEJ) process to repair DSB that is error prone leading to higher risk of genetic instability.[35-38] However, it is not known if during reprogramming normal somatic cells to human iPSC if *CYCLIN D1* repairs DSB preferentially via HR.

Therefore, we next assessed early passage 2 human iPSC (early), passage 10 (established) cells, and NSC derived from the iPSC for RAD51 protein expression. RAD51 is a standard marker of DNA repair by HR and nuclear localization of RAD51 protein is essential for DNA repair by HR.[41-43] Interestingly, RAD51 protein is localized mostly in the nucleus of DH-iPSC (Figure 3A,B). In contrast, MH-iPSC RAD51 is localized predominantly in the cytoplasm, where RAD51 cannot repair DSB by HR (Figure 3A,B). Given it is well established in normal cells that nuclear localization of RAD51 protein expression is essential for DNA repair by HR,[42] suggests that *CYCLIN D1* is repairing DSB during cell reprogramming by HR.

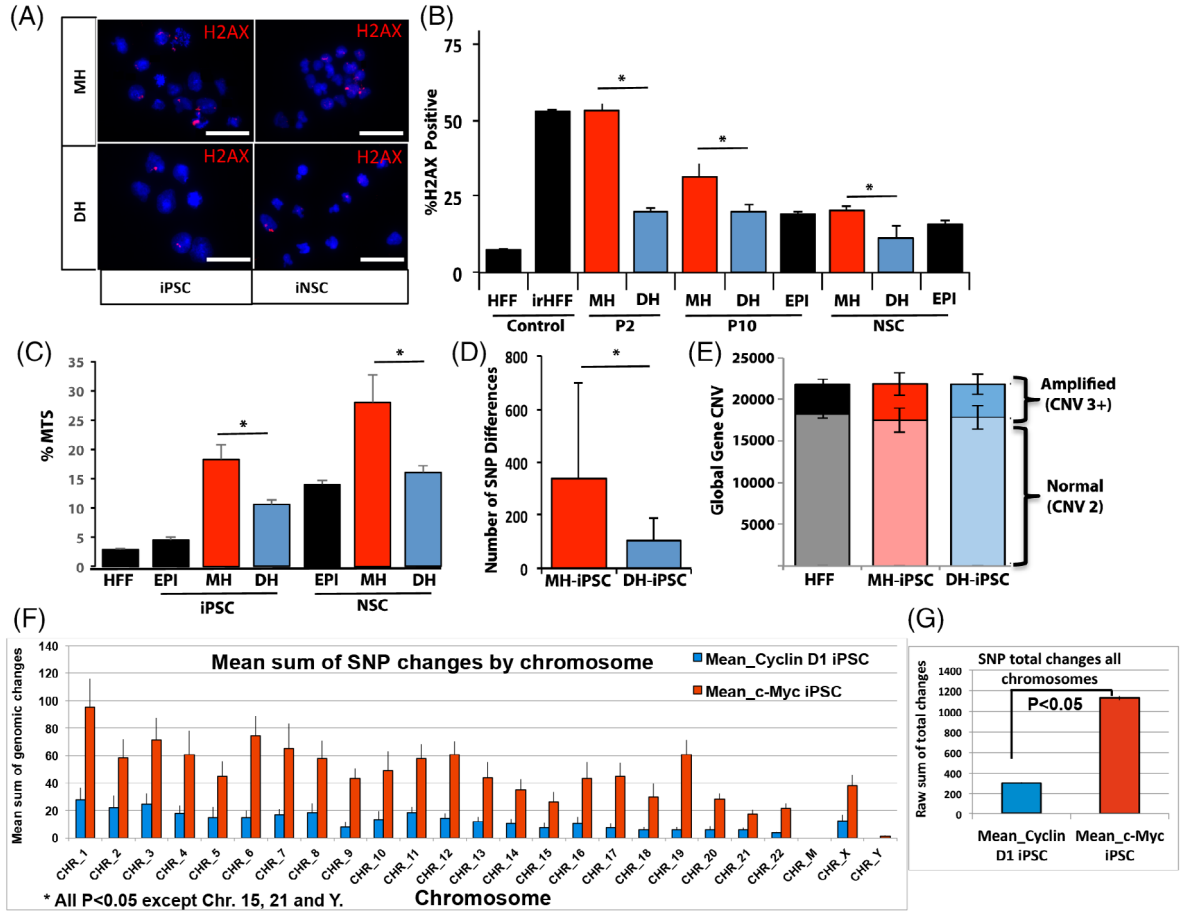

(H)

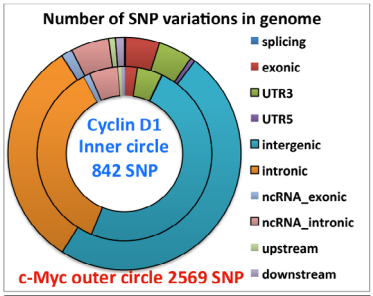

	Cyclin D1 iPSC	c-Myc iPSC
Region of Genome	# SNP variations	# SNP variations
splicing	1	4
exonic *	19	121
UTR3	39	123
UTR5	1	17
intergenic	413	1248
intronic	304	821
ncRNA_exonic	10	40
ncRNA_intronic	45	136
upstream	5	24
downstream	5	32
Total general	842	2569

*Exonic region P<0.05

(I) Cancer genes with SNP and Chromosome location

Cyclin D1 iPSC		c-Myc iPSC	
Gene name	Chr location	Gene name	Chr location
EREG	*Chr 4 UTR3*	TNFRSF10B	*Chr 8 UTR3*
NTRK3	*Chr15 UTR3*	PTCH1	*Chr 9 UTR3*
PDGFRL	*Chr 8 exonic*	PDGFRL	*Chr 8 exonic*
RPS29	*Chr 14 UTR3*	RHOBTB2	*Chr 8 UTR3*
VAV2	*Chr 9 exonic*	SHCBP12	*Chr 1 Exonic*
PDGFRL	*Chr 8 exonic*	CYP2E1	*Chr 10 Splicing*
TLR4	*Chr 9 exonic*	DUSP3	*Chr 17 UTR3*
SCTR	*Chr 2 exonic*	GALNT	*Chr 1 UTR3*
TOTAL	8 cancer genes	FZD10	*Chr 12 Exonic*
		HOXB2	*Chr 17 UTR3*
		NTN1	*Chr 17 UTR3*
		NCOR2	*Chr 12 Exonic*
		C1orf56	*Chr 1 Exonic*
		MGAT4B	*Chr 5 UTR5*
		AKAP13	*Chr 15 Exonic*
		CBLC	*Chr 19 Exonic*
		ETV7	*Chr 6 Exonic*
		MYO18B	*Chr 22 Exonic*
		TOTAL	18 cancer genes

FIGURE 2 *CYCLIN D1* reprogrammed iPSC have improved genomic stability. A, Photos of immune-staining for H2AX signal of human induced pluripotent stem cells (iPSC) and neural stem cells (NSC) generated with *C-MYC* (MH) or *CYCLIN D1* (DH) compared with commercially available episomal made iPSC and NSC. Nuclei stained with 4′,6-diamidino-2-phenylindole (DAPI). B, Graph of quantification of percent of cells with H2AX signal (*X*-axis) during the reprogramming process compared with parental human foreskin fibroblasts (HFF) cells and differentiated NSC (*$P \leq .05$). C, Graph of quantification of percent of cells with multitelomere signal (MTS) (*$P \leq .05$). See Figure S7B for photos of MTS. D, Graph of quantification of global SNP changes as determined by infinium Omni5-4 v1.2 array. Not significantly different (SD) between HFF and iPSC. E, Graph of quantification of global copy number variation (CNV) changes from the SNP array data. Not SD. F, Graph of quantification of SNP changes per chromosome demonstrating less SNP changes in *CYCLIN D1* made iPSC (*$P \leq .05$). G, Graph of quantification of all SNP changes (0, 1, or 2) per chromosome demonstrating less SNP changes in *CYCLIN D1* made iPSC. G, Graph of the location of SNP changes (0, 1, or 2) in the genome for *C-MYC* (outer circle indicating more changes) or *CYCLIN D1* (inner circle indicating less changes) generated iPSC. I, Table of names and number of cancer-related genes with SNP changes (0, 1, or 2) for *C-MYC* (18 cancer-related genes) or *CYCLIN D1* (8 cancer-related genes) generated iPSC with chromosome location and genetic region affected. n = 3 *C-MYC* clones and n = 3 *CYCLIN D1* clones for all figures

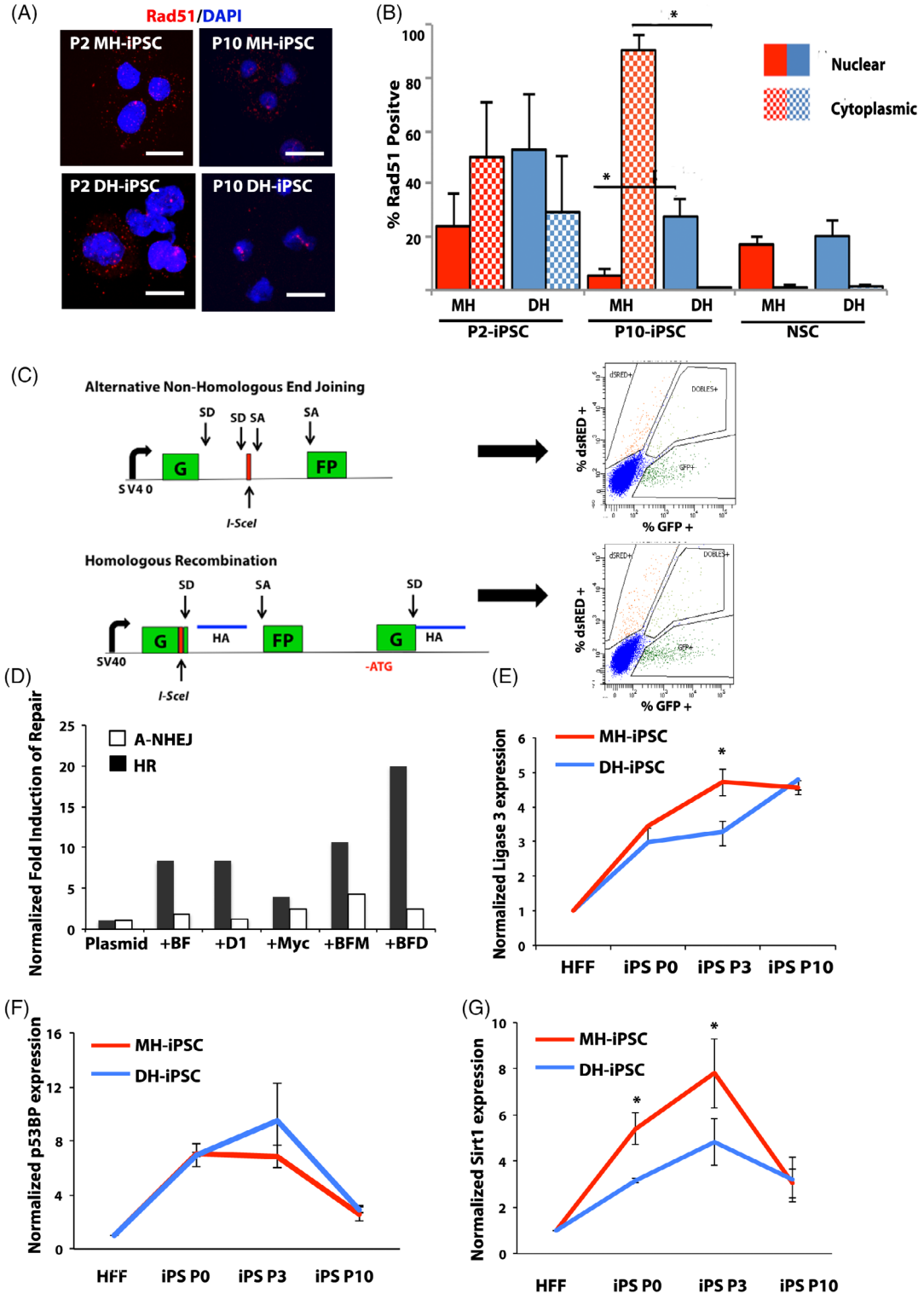

FIGURE 3 *CYCLIN D1* reprogrammed cells preferentially repair DNA through homologous recombination. A, Localization of RAD51 protein (red) by immunofluorescence. 4′,6-diamidino-2-phenylindole (DAPI)-stained nuclei in blue. B, Quantification of RAD51 protein localization exclusively in the nucleus or cytoplasm at P2 (early), P10 (established) and in iPSC-derived NSC (*$P \leq .05$). C, Schematic of DNA repair reporter constructs. D, Quantification of flow cytometry for homologous recombination (HR) or Alternative NHEJ GFP reporter constructs experiments in phoenix cells under cell reprogramming conditions (*OCT3/4*, *SOX2*, *KLF4* alone, or plus *CYCLIN D1* or *C-MYC*) demonstrates a preference for HR in cells reprogramming with *CYCLIN D1* and a preference of Alternative NHEJ in cells reprogramming with *C-MYC*. Representative of three experiments: E, Q-RT-PCR for *LIGASE 3* mRNA levels (*$P \leq .05$); F, Q-RT-PCR for *p53BP* mRNA levels, not SD; G, RT-PCR for *SIRT1* mRNA levels (*$P \leq .05$)

To confirm that DH-iPSC have enhanced DNA damage repair and a preference toward the HR pathway under cell reprogramming conditions (cells transfected to overexpress reprogramming factors *OCT3/4*, *SOX2*, *KLF4* alone or with *CYCLIN D1* or *C-MYC*), we used GFP reporter plasmids that allow GFP expression exclusively via either the HR or alternative NHEJ pathways and measured the level of GFP activity by flow cytometry (Figures 3C,D and S8).[44] Under reprogramming conditions with *CYCLIN D1*, cells preferentially repair DSB by HR, whereas *C-MYC* preferentially activates the alternative NHEJ process (Figures 3D and S8). Lastly, to demonstrate further that MH-iPSC preferentially repair DSBs via the alternative NHEJ pathway during reprogramming to human iPSC we measured *LIGASE 3* gene expression levels during the cell reprogramming process in starting parent cells (HFF), passage 0 (very early), passage 3 (early), and passage 10 (established). *LIGASE 3*, a gene marker of the alternative NHEJ process, was found in MH-iPSC to have significantly higher levels of gene expression at the early passage 3 confirming the reporter based assay that MH-iPSC repair DSB predominately by alternative NHEJ (Figure 3E).

We next assessed expression of significant genes found to be involved in DNA damage response and general cell stress during the cell reprogramming process in starting parent cells (HFF), passage 0 (very early), passage 3 (early), and passage 10 (established). Specifically we examined by RT-PCR gene expression levels of: (a) DNA damage response gene *53BP1*; (b) apoptosis inhibition related gene *IAP2*; and (c) general cell stress genes *SIRTUIN* 1 and 6. Passage 0 human iPSC mRNA was obtained from scraping multiple clones for MH and DH hiPSC that were left over from picking clones for expansion at the 2-week stage of reprogramming. Also, three MH and DH iPSC clones were assessed for each condition at passage 3 (early) and passage 10 (established) and compared with HFF parental starting cells to capture the reprogramming process. The data revealed only *SIRT1* was significantly different between MH and DH hiPSC over time (Figures 3F,G and S9). Interestingly, a "window" of reduced cell stress (lower *SIRT1* induction) was observed for DH hiPSC clones from passage 0 hiPSC until passage 10, when hiPSC are considered a mature stable cell line (Figure 3G). Taken together, the data demonstrate that *CYCLIN D1* repairs DSB via HR during the reprogramming process to hiPSC with reduced general cell stress levels that results in significantly improved genetically stable hiPSC clones.

2.4 | *Cyclin D1* promotes reprogramming in mouse cells and rescues requirement for *Sirt1*

To validate the role of *Cyclin D1* in another cell line and species we generated mouse iPSC and assessed DNA damage levels and genetic stability (Figure 4). We made mouse iPSC using retroviral methods and tested efficiency of reprogramming by colony formation assay using three conditions: 3F (*Oct3/4*, *Sox2*, *Klf4*) alone, 3F plus *c-Myc*, and 3F plus *Cyclin D1*, compared with mouse ESC (mESC). 3F alone produced a low number of early iPSC colonies; however, 3F plus *Cyclin D1* was significantly more efficient than 3F+*c-Myc*, generating more AP-positive colonies at the 2-week time point (Figure 4A). 3F plus *c-Myc* reached similar levels of colony number at the 3-week time point (*P* value = .0062) (Figure 4C). To ensure proper protein expression was achieved, *Oct3/4* and *Cyclin D1* protein levels were assessed by Western blot and were both confirmed in iPSC clones (Figure S10A,B).

Next, we assessed DSB encountered during reprogramming mouse cells using the H2AX staining and observed significantly lower levels of H2AX signal in 3F plus *Cyclin D1* made iPSC compared with iPSC made with *c-Myc*, consistent with the results in human cells (Figure 4D-F). To assess genomic stability of mouse iPSC made with 3F plus *c-Myc* or *Cyclin D1*, we analyzed telomere length using the quantitative telomere FISH (Q-FISH) assay. We observed that 3F plus *Cyclin D1* clones had a decrease of signal-free ends, 4.19% to 1.91% compared with 3F plus *c-Myc* clones, demonstrating a decrease in telomere instability footprint with *Cyclin D1* made mouse iPSC (Figure 4G-I).

To determine if *Cyclin D1* with 3F reduces cell stress during cell reprograming, we tested by RT-PCR the expression of a panel of DNA damage and cell stress gene markers: (a) *ATM*, *53BP1* and *MnSOD* for DNA damage response; (b) apoptosis inhibition related genes *IAP2* and *GADD45b*; and (c) cell stress response genes *Sirtuin 1*, *3*, and *6* (Figures 4J and S10C). Mouse C2C12 cells were used as a negative control and mESC as a positive control of pluripotency. Three clones for every condition (3F plus *c-Myc* and 3F plus *Cyclin D1*) were compared at passage 1 and passage 5. 3F alone were not analyzed due to low efficiency and high cell death observed (Figure 4C). The iPSC clones reprogrammed with 3F plus *c-Myc* expressed higher levels of *IAP2* (*P* value = .0184) (Figure S10C). *Gadd45b* (*P* value = .0342) (Figure S10C) and *Sirt1* (Figure 4J; *P* value = .01) than clones reprogrammed with 3F plus *Cyclin D1*, while other DNA damage, apoptosis or cell stress gene markers were not significantly different over time (Figure S10C). The data confirm the human cell reprogramming data that 3F plus *Cyclin D1* is an efficient method with suppressed DNA damage/cell stress pathways when compared with the classical 3F plus *c-Myc* method during murine cell reprogramming to iPSC.

We next sought to focus on the role of *Cyclin D1* in reprogramming with *Sirt1*, a gene associated with general cell stress, genetic stability and cell reprogramming efficiency. Recently, in mouse iPSC, *Sirt1* has been described as necessary for proficient telomere elongation and genomic stability of iPSC made with *c-Myc*.[45] We reprogrammed *wild type* and *Sirt1* null mouse embryonic fibroblasts (*WT and Sirt1−/−* MEFs) with the conditions: 3F alone; 3F plus *c-Myc*; or 3F plus *Cyclin D1*. Analysis of AP staining of reprogramming colonies demonstrated that the combination of *Sirt1−/−* MEFs with 3F plus *c-Myc* was unable to reprogram to iPSC (*P* value = .04), suggesting that *Sirt1* is essential to rescue the cell stress induced by *c-Myc* during cell reprogramming (Figure 4K). However, 3F plus *Cyclin D1* was able to reprogram cells to iPSC independent of *Sirt1*, demonstrating that *Sirt1* is not essential for 3F plus *Cyclin D1* reprogramming to pluripotency (Figure 4K).

3 | DISCUSSION

The development of a clinically compatible method to reliably generate genomically stable human iPSC is essential for cost-effective

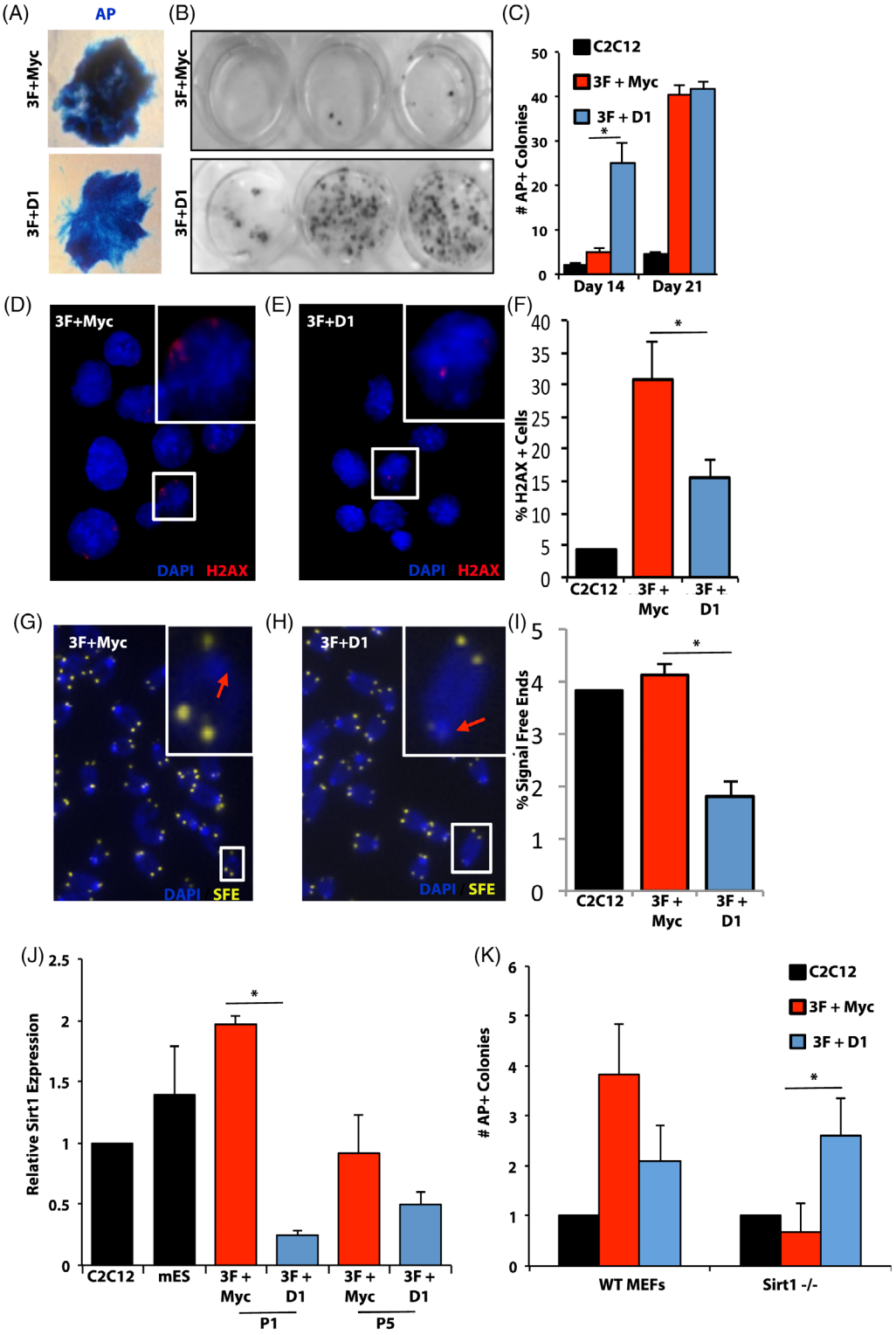

FIGURE 4 Mouse induced pluripotent stem cells (iPSC) reprogrammed with three factors and *Cyclin D1* rescues requirement for *Sirt1* and reduces genetic instability. A, *Cyclin D1* or *c-Myc* plus three factors reprogram to alkaline phosphatase (AP) cells. B, Bright field of three representative experiments stained for alkaline phosphatase (AP). C, Quantification of AP+ colonies at days 14 and 21 of reprogramming (*$P \leq .05$). D,E, Cells stained for nuclei (4′,6-diamidino-2-phenylindole [DAPI]; blue) and double-strand breaks (H2AX; red). F, Quantification of H2AX-positive nuclei (*$P \leq .05$). G,H, Cells stained for multiple telomere signal (MTS; yellow) and nuclei (DAPI; blue). I, Quantification of MTS (n = 3 clones each) (*$P \leq .05$). J, Q-RT-PCR for *Sirt1* expression levels at P1 and P5 for selected mouse iPSC clones and mouse embryonic stem cells (mESC) (n = 3) (*$P \leq .05$). K, Quantification of AP+ colonies in WT and SIRT1−/− MEFS (*$P \leq .05$)

clinical applications and accurate disease modeling. Developing stringent guidelines to take into consideration the long-term 5- to 10-year effects of transplanted iPSC-derived cells essential for its long-term success. Key to these issues is the repair of DNA damage during the reprogramming process to improve genetic stability of human iPSC. Here, we take advantage of the DNA repair promoting function of *CYCLIN D1* to describe an improved clinically compatible method to reprogram human cells for clinical applications. We adopt a feeder-free synthetic mRNA transfection and produce high quality human iPSC with reduced cell stress, reduced genetic instability, and that engraft successfully in vivo from clinically easy-to-access cells. With improved genetically stable hiPSC, we used clinically compatible cell culture system (Thermo Fisher) to establish a protocol that could be easily applied for generating clinical-grade human hiPSC in good manufacturing practice cell culture rooms. Although in development, there is currently no internationally agreed SOP for generating clinical grade human iPSC, the addition of synthetic mRNA transfection methods and the use of *CYCLIN D1* in the reprogramming method would reduce long-term risks and overall improve the method for clinical applications.

The RIKEN clinical trial that used human iPSC generated with four factors and that includes *C-MYC* has revealed issues with genomic instability, calling for a method to generate hiPSC that will give more reliable outcomes with less genetic instability or threat of pathology to ensure long-term stability of transplanted cells.[21,22] Assessment of proliferation levels in teratomas are significantly reduced in *CYCLIN D1* made iPSC compared with *C-MYC* iPSC (Figure 1I). Here we found that NSC generated from *CYCLIN D1* synthetic mRNA made iPSC-NSC engraft and survive in the hostile spinal cord injured damaged tissue microenvironment with proper differentiation and no evidence of neoplastic growth (Figure 1C). Long-term studies were required to fully rule out the potential of tumorigenicity from these cells and highlights that utilizing *CYCLIN D1* made iPSC and derivative cells for transplantation represent a safer method for clinical applications. Further research is warranted to explore the regenerative capacity of NSC to treat SCI and recent work holds great promise.[46,47]

Characterization of human iPSC clones using standard methods found no difference between commercially available hiPSC made with episomal methods, MH and DH hiPSC (Figure 1). Interestingly, no significant increase in global CNV was observed compared with starting parental HFF cells, supporting other work that suggests the synthetic mRNA method is the best method for generating genetically stable iPSC[16] (Figure 2). Deeper analysis of the Omini5.2 SNP array data found that DH iPSC have significantly different less SNPs per chromosome, except for chromosomes: 16, 21 and Y (Figure 2F,G and Table 1). Further analysis of the hiPSC for DNA damage and cell stress levels occurring during iPSC formation using *CYCLIN D1* demonstrated a window of reduced cell stress compared with using *C-MYC*, implicating *SIRT1* (Figure 3G). Functional analysis of *Sirt1* null mouse cells during reprogramming demonstrated that *Cyclin D1* is able to reprogram cells to mouse iPSC independent of *Sirt1*, while three factors plus *c-Myc* need *Sirt1* for reprogramming (Figure 4J,K). The role of *Sirt1* in miPSC is thought to be essential to facilitate miPSC generation through de-acetylation of *p53*, inhibition of *p21*, and enhancement of *Nanog* expression.[48] Recently, *Sirt1* has been described as necessary for proficient telomere elongation and genomic stability of iPSC made with *c-Myc*.[45] We demonstrate that *Cyclin D1* is able to reprogram cells to miPSC without *Sirt1*, suggesting *Cyclin D1* is able to replace the *Sirt1* role to maintain efficiency during reprogramming to iPSC (Figure 4J).

TABLE 1 Quantification of global gene CNVs

	HFF	MH-iPSC	DH-iPSC
Amplifications	3558.4	4379.7	3971.4
Normal	18 278.2	17 511.0	17 873.0
Deletions	0.8	1.3	1.0

Abbreviations: CNV, copy number variation; HFF, human foreskin fibroblasts; iPSC, induced pluripotent stem cells.

CYCLIN D1 reduces the genetic instability footprint in human iPSC and iPSC-derived NSC as demonstrated by multiple aspects of genomic instability of a cell: (a) reduced MTS; (b) lower H2AX signal, that is, lower DSB in iPSC and derived NSC; (c) correct nuclear localization of Rad51 protein; (d) reduced SNP changes per chromosome (Figure 2A-G). A direct role for *CYCLIN D1* in promoting repair of DSB via *BRCA2* and *RAD51* is well established in normal or cancer cells via the HR pathway.[31,34] We observed that *CYCLIN D1* acts to enhance DNA damage repair during reprograming in contrast to *C-MYC* made iPSC that have almost exclusively RAD51 localized to the cytoplasm during reprogramming, leaving DSB inefficiently repaired by alternative NHEJ (Figure 3A,B). It is highly likely that during the early cell reprogramming process *CYCLIN D1* acts to enhance DNA damage repair by facilitating RAD51 filament formation in the nucleus resulting in a reduced footprint of DNA damage (lower H2AX) that persists to passage 10 iPSC and even NSC. This suggests an epigenetic effect, such as DNA methylation that warrants further investigation.

The use of other cell types, such as cord blood cells that can be reprogramed with fewer reprogramming factors is hindered by the fact they are: (a) harder to access clinically, (b) technically demanding to culture, (c) can only be reprogrammed by viral methods (including Sendai virus), and (d) would allow only an allogeneic HLA-matched treatment approach. However, using *CYCLIN D1* in the reprogramming cocktail to reprogram cord blood cells could repair DNA damage caused by conventional cell reprogramming methods using c-Myc and improve the probability of generating better genetically stable hiPSC clones for cell banking purposes and reduce risk of removing patients in future clinical applications for genomic instability.

In conclusion, the reliability of long-term clinical trials to treat human disease with hiPSC-derived cells is dependent on the quality of the starting hiPSC. We describe a new method adopting synthetic mRNA reprogramming methods using *CYCLIN D1* that repairs DNA during cell reprogramming by HR to generate improved genomically stable hiPSC and iNSC with reduced teratoma cell proliferation, low CNV, and long-term survival with proper differentiation in a hostile microenvironment that could be developed for current and future clinical applications to model and treat human disease. Further testing of the

CYCLIN D1 reprogramming method to reduce DNA damage and increase genetic stability using other cell types is warranted. Stringent guidelines including assessment of genetic stability of iPSC need to be taken into consideration for the long-term clinical success of transplanted iPSC-derived cell strategies and disease modeling studies.

4 | MATERIALS AND METHODS

Part of the materials and methods appear in the PhD thesis of Jordi Requena Osete and the Masters thesis of Carme Grau-Bove, University of Barcelona (https://www.tdx.cat/handle/10803/457970#page=1).

4.1 | Cell culture

Mouse C2C12 cells were obtained from ATCC (CRL-1772). Mouse embryonic fibroblasts were obtained from embryos of pregnant mice Wild Black6, C57 strain, at day 12.5 postcoitum (extraction protocol approved by the University of Barcelona Ethics Committee). All mouse iPSC and mESC were cultured in G4 medium: knockout (KO)-Dulbecco's modified Eagle's medium (DMEM; Gibco, Carlsbad, California, # 10829-018) supplemented with glutamate 1%, penicillin-streptomycin 1%, fetal bovine serum 15%, nonessential amino acids 1% (NEM-NEAA 100× Gibco), sodium pyruvate 1% (Gibco # 11360), 2-mercaptoethanol 0.2%, the cytokine *leukemia inhibitory factor* (LIF) 0.02% (Chemicon # ES61107, 1.000 U/mL) and 2 mM valproic acid (Sigma-Aldrich, 1069-66-5). In order to arrest MEFs to prepare feeder layer, cells were treated with Mytomicin C during 4 hours or irradiated with gamma irradiation. Mouse iPSC were maintained on irradiated MEFs (irMEFs) in G4 medium: *Human*: HFF were obtained from MERCK (SCC058, Lote NRG1000064). Retrovirally made hiPSC were maintained on irradiated HFF (irHFFs) in hES medium consisting of KO-DMEM, 1 mM pen/strep, 1 mM Gluta-MAX, 1× nonessential amino acids, 55 μM β-mercaptoethanol (Gibco), 10% KO serum replacement (Invitrogen, Carlsbad, California), and 10 ng/mL FGF2 (R&D Systems Inc., Minneapolis, Minnesota). For maintenance of undifferentiated colonies, differentiated cells were manually removed and undifferentiated cells were passaged once a week. Feeder-free clinical grade mRNA iPSC were cultured in Flex E8 culture medium (Life Technologies, A2858501) on Vitronectin (Life Technologies, A14700)-coated plates.

4.2 | Generation of mouse iPSC by retroviral infection

For mouse reprogramming experiments, 50 000 or 100 000 cells were seeded per well of a six-well plate and infected with retroviral supernatants of a polycistronic retroviral vector containing three factors (3F) *Oct4*, *Sox2*, *Klf4*, and *GFP* as a reporter gene (pPMXS-OSKG). Then, either pMSCV-*c-Myc* or p-Babe puro *Cyclin D1* was added to 3F to generate 3F plus *c-Myc* or 3F plus *Cyclin D1*, respectively. Retroviruses for the different factors were produced using phoenix ecotropic packaging cell line in order to produce viral supernatant with virus to infect mouse cells and human cells. After 24 hours, DMEM was replaced, cells were incubated at 32°C, and viral supernatant was harvested after 24 and 48 hours. Infection consisted of a 45-minute supernatant spinfection at 750*g* in the presence of 1 mg/mL polybrene. Three rounds of infections on consecutive days were performed. Two days after beginning the last round of infection, cells were trypsinized and seeded onto feeder layers of irradiated MEFs. The medium was changed upon platting to G4 with LIF for mouse iPSC. Cultures were maintained at 37°C, 5% CO_2, changing medium every other day.

4.3 | Synthetic mRNA reprogramming to iPSC

Human iPSC ethics was applied for approved projects Maraton TV3 2018 (2020/00298/P1); BFU2011-26596. Reprogramming method was performed using Stemgent's microRNA-enhanced mRNA reprogramming kit (STEMGENT, #00-0071) protocol including Oct4, Sox2, Klf4, and Lin28 with or without c-Myc or *CYCLIN D1* mRNA. Messenger RNA used for transfections are included in Stemgent kit, minus *CYCLIN D1* mRNA was synthetized by in vitro transcription (IVT) using the MEGAscript Kit (Ambion, #AM1334). DNA template for the mRNA IVT for *CYCLIN D1* was made by cloning *CYCLIN D1* ORF between the 3′ and 5′ untranslated regions of alpha-globin by splint ligation to increase the stability and translation efficiency of the transcript. *CYCLIN D1* DNA template was used to synthesize the messenger RNA by IVT. IVT was performed using mMessage mMachine kit (AM1344 Thermofisher) adding pseudouridine and 5-mehtyl-cystidine (Trilink) to replace uridine and cystidine in the nucleotide mix and adding antireverse CAP analog (Trilink). *CYCLIN D1* mRNA was functionally tested by counting the % 5-ethynyl-2-deoxyuridine-positive cells after 24 hours in low serum and transfecting HFFs with different amounts of mRNA (Figure S2). RNase and DNase free tubes and tips were used, gloves and working surface treated with RNaseZap (Sigma, #R2020). For the cells transfection, briefly, HFFs were seeded on vitronectin-coated 24 multiwell plate wells at six different densities: 7.5k, 10k, 12.5k, 15k, 17.5k, and 20k. The next day, three densities with 50% to 70% confluence were selected. Transfections were done in cells cultured in Pluriton medium (Stemgent #00-0070), adding 300 ng B18R/mL to inhibit immune response to transfected material. Pluriton medium was conditioned 24 hours before on irHFFs the day before adding it to the target HFFs to be transfected. MicroRNA and mRNAs were transfected as indicated by the manufacturer's protocol using Stemgent transfection reagent (STEMGENT, #00-0071). Messenger RNA cocktail was transfected at a stoichiometric proportion of 3:1:1:1:1 of the reprogramming genes: *OCT4*, *SOX2*, *KLF4*, *LIN28*, and *C-MYC* or 50 ng of *CYCLIN D1* (OSKM or OSKD). Two hundred nanograms of mRNA were transfected per well of a 24 MW plate. MicroRNA was transfected at days 0 and 4, and mRNA from days 1 to 12. At days 14-15 colonies were picked by mechanically scrapping them and were transferred to Vitronectin coated plates in Conditioned

Pluriton mixed 1:1 with E8 medium. Rho kinase inhibitor (ROCKi, Y-27632, STEMCELL Technologies #72302) was added at 10 μM final concentration during the first 24 hours after colony picking to prevent cell apoptosis. Medium was change to E8 (not feeder conditioned and with no Pluriton) 24 hours later and refreshed daily. Colonies were passaged by gentle dissociation with 0.5 mM Ethylenediaminetetraacetic Acid (EDTA) when they were 75% to 80% confluence. Episomal-made iPSC were purchased (Life Technology) and maintained on vitronectina-coated plates in Essential 8 (E8) medium.

4.4 | In vitro differentiation

Mouse and human iPSC general differentiation was carried out by plating embryoid body on gelatin and DMEM (Life Technologies 21969035), with 20% fetal calf serum changed every second day for 2 to 3 weeks. Human iPSC in vitro guided differentiation toward endoderm, mesoderm, and ectoderm was done using PSC Neural Induction Medium kit (Life Technologies, A1647801) for NSC coating the plates with Geltrex (Life Technologies, A1413201). CM differentiation was done using PSC Cardiomyocyte Differentiation kit (Life Technologies, A2921201) and CM kept in culture until beating was stable. DE was differentiated from iPSC using PSC DE Induction kit (Life Technologies, A27654SA). As an internal control for all the differentiation protocols, we differentiated in parallel a commercial Episomal made iPSC (Life Technologies, A18945).

4.5 | Teratoma formation

Animal experiments were approved by the University of Barcelona ethics committee. Two million cells were subcutaneously injected at the flank of athymic FoxN1 nu/nu mice (ENVIGO). After 3 to 4 months, teratomas were extirpated and fixed in paraformaldehyde 4% O/N. Next day teratomas were embedded in paraffin and sections were analyzed for H&E staining to recognize germ layer structures and for KI-67 staining to assess the in vivo tumorigenic potential of injected iPSC.

4.6 | Immunocytochemistry and flow cytometry for pluripotency and differentiation

Cells were grown on plastic cover slide chambers and fixed with 4% paraformaldehyde (PFA). After fixation and washing, cells were blocked with phosphate-buffered saline (PBS) containing 6% donkey serum, and 0.5% Triton X-100 for 30 minutes. Cells were then stained for appropriate markers described in the figures. Pluripotency markers: anti-Oct4 (Santa Cruz, sc-5279, 1:60), anti-Sox2 (CalBiochem, sc1002, 1:100) anti-SSEA3 (Abcam MC631, ab16286, 1:10), anti-SSEA4 (Hybridoma bank, MC-813-70, 1:50), and anti-Tra-1-81 (Abcam ab16289, 1:300). For generally differentiated cells immunofluorescence was performed for endoderm marker anti-AFP (Dako, A0008, 1:400), mesoderm marker anti-αSMA (Sigma, A5228-100) and ectoderm marker anti-Tuj1 (Biolegend, MMS-435P-100, 1:500). Primary antibodies for guided differentiation into cardiomyocyte markers: anti-cardiac troponin T (Abcam, ab10214, 1:400) and anti-Gata4 (Santa Cruz, sc-9053, 1:200); neuronal markers: anti-nestin (Biolegend, 841801, 1:200), anti-MAP2 (R&D systems, MAB8304, 1:250); endoderm cells were analyzed with anti-hCXCR4 PE conjugated (FAB173P). Secondary antibodies used were all the Alexa Fluor Series from Invitrogen (diluted 1:200). Images were taken using a Leica SP5 confocal microscope. During confocal microscopic observation, all the images were taken using the same settings. Tile scan image imaging was performed with an AF6000 Epifluorescence microscope for SCI spinal cord immunofluorescence stained sections. All flow cytometry analysis was performed on a FACS Canto II machine.

4.7 | DNA damage GFP reporter plasmid methods

Previously designed and published HR and alt NHEJ plasmids were used and are available upon request (44). Ten micrograms of plasmids (288 ng/μL) were digested with ScI-I overnight at 37°C and a 1% agarose used to check complete digestion. DNA was purified by isolate II PCR and gel Kit (Bioline) in 30 μL, with approximately 50% recovery assessed by Qubit^R dsDNA BR assay kit and Qubit^R 2.0 flurometer (Life Technologies). Phoenix cells were cultured in DMEM with 10% fetal bovine serum, Pen/Strep, and Glutamaxl (Gibco 35050061). Cells were transfected in 12 well plates at 80% to 90% of confluence with Lipofectamine 3000 (Life Technologies L3000015) with the following samples: GFP, circular and linearized plasmids: 900 ng, 3F (Oct4/Sox2/Klf4): 450 ng, DsRED: 50 ng, C-MYC 150 ng or cycling D1, 150 ng.

4.8 | AP staining and Western blot

Pluripotent stem cells present high levels of AP enzyme. AP Blue Membrane Substrate Solution (AB0300-1KT) was used to detect iPSC AP expression levels as a standard assay. For Western blot analysis, resolving Sodium dodecyl sulfate (SDS) gels were used and nitrocellulose membranes were blotted overnight at 4°C with anti-Oct4 (Santa Cruz Biotechnology, Inc, sc-5279, 1:100), anti-CYCLIN D1 (Santa Cruz, sc753, 1:500), developed with appropriate secondary anti-mouse and anti-rabbit HRP antibodies and developed with Advansta Western-Bright ECL.

4.9 | Karyotype analysis

In order to see chromosome G bands, methanol: acetic acid (3:1) fixed cells were stained with Wright: Sorensen buffer (1:3). Twenty metaphases were assessed per sample and chromosomes were classified using Ikaros software.

4.10 | Telomere length and cytogenetic analysis using telomere Q-FISH on metaphases

Cells were incubated with 0.1 μg/mL colcemide (Gibco) for 4 hours at 37°C, swollen in hypotonic buffer (sodium citrate 0.03 M) for 25 to 45 minutes and then fixed in methanol:acetic acid (3:1). Cells were concentrated and 30 μl were dropped onto slides falling from 10 cm high. After washing, metaphase spreads were fixed in 4% formaldehyde in PBS, and Fluorescence in situ hybridization (FISH) was performed as described previously,[45] using a telomere probe (Panagene, Cy3-TEL). For analysis of chromosomal aberrations, metaphases were analyzed by superimposing the telomere image on the 4′,6-diamidino-2-phenylindole (DAPI) image using TFL-telo software.

4.11 | Rad51 and H2AX DSB immunofluorescence staining

Methanol: acetic fixed cells were stained for anti-gamma H2AX (Ser139) antibody (Novus, NB100-78356-0.025, 1:500) to determine the percentage of DSBs and Rad51 localization (1:500). Cells were blocked in PBS, 2% Donkey serum, 0.05% Triton-X100. Primary antibody was incubated o/n at 4°C. Secondary antibody, goat anti-mouse A568 (A11031), was incubated 1:200 for 2 hours at 37°C. Quantification was performed using ImageJ by counting H2AX or Rad51-positive foci in 200 nuclei per experiment.

4.12 | CNV analysis

CNV was analyzed with the Infinium Omni5-4 v1.2 Kit (20005150) from Illumina. The genotyping array was processed following manufacturer's instructions. Briefly, 400 ng of genomic DNA were used as input material, arranging the different samples in random order in the odd columns of a 96 well plate. Genomic DNA was subjected to a whole genome amplification reaction, followed by end-point enzymatic fragmentation and precipitation of the DNA. Resuspension hybridization and wash solution (RA1) was used to resuspend the precipitated DNA, and load it into the microarrays for a 16-hour hybridization step carried at 48°C. After the incubation step, unhybridized DNA molecules were washed away with PB1 buffer, and arrays were assemble in Flow-Through chambers, in order to perform the X-staining step were a single-base extension followed by an inmunofluorescent labeling enabled the interrogation of the 4.284.426 markers. Data acquisition from the processed genotyping microarrays was carried out with an iScan scanner. GenomeStudio software (v2.0.0.476) was used with its genotyping module (v2.0.0) to perform the genotype calling using the provided cluster file for this product (HumanOmni5M-4v1_B). Copy number analysis was carried out with cnvPartition GenomeStudio add-in (v3.2.0), with default parameters (confidence threshold = 35; Detect Extended Homozygosity = True, minimum probe count = 3).

4.13 | Microarray analysis

RNA quality control: The quantity and quality of isolated RNAs were determined with a NanoDrop ND-1000 (NanoDrop Technologies, Wilmington, Delaware) and a Bioanalyzer 2100 (Agilent, Waldbronn, Germany). The RNA integrity numbers (RIN) in all cases ranged from 9.4 to 10, thereby indicating minimal RNA degradation. *Microarray Analysis*: Three biological replicates of human iPSC lines generated with *C-MYC* (MH) or *CYCLIN D1* (DH), plus samples of the episomal made human iPSC line and HFF fibroblasts were analyzed for differential gene expression by microarray hybridization. For each sample, 500 ng of total RNA with spike-in controls added were labeled using Agilent's Low input quick Amp Labeling kit, by mRNA reverse transcription with T7-oligo-dT primer followed by IVT with T7 RNA polymerase in the presence of Cy3-CTP. The labeled cRNAs were hybridized to 60-mer oligo microarrays (SurePrint G3 HumanV3 GE 8x60K Microarray, Agilent microarray design ID 072363) according to the manufacturer's one color protocol (Version 6.5, May 2010). The arrays were scanned on an Agilent G2565BA microarray scanner at 100% PMT and 3 μm resolution. Data were extracted using Feature Extraction (Agilent) software. *Statistical Processing*: Hybridization intensities were background corrected with normexp and normalized by quantile normalization. Log2ratio values were computed for MH and DH vs HFF samples. Per-probe log2ratios were aggregated to per-gene values by taking median values. Signal processing and analysis for differential expression on a gene-by-gene basis was performed by linear models and empirical Bayes methods.[49] Correction for multiple testing was performed using the False Discovery Rate (FDR) method. The list of regulated genes was brought into biological context by gene set enrichment analysis using GSEA.[50] We used the pre-ranked mode with default settings (weighted enrichment statistic) using the average log2ratio as ranking metric and tested for enrichment in literature datasets against the version 6.1 C2cgp chemical and genetic perturbation gene set collection from MaSigDB. hESC gene expression profile used by Ben-Porath et al.[51]

4.14 | Real-time PCR

Total mRNA was isolated using Ambion RNA purification columns kit (#12183018), and 500 ng was used to synthesize cDNA using the SensiFAST cDNA synthesis kit (Bioline, BIO65053). One microliter of the reaction was used to quantify gene expression by quantitative PCR as previously described.[4,29]

Primers sequences are listed in the table below:

4.15 | Spinal cord contusion, NSC transplantation

Sprague Dawley female rats with average weight of 200 g were subjected to complete spinal cord section using a hook and an iridectomy scissor, at thoracic segment T8 after partial laminectomy from T7 to T9. For intramedullary transplantation, 2×10^6 iNPC were transplanted by stereotaxis distributed into rostral and caudal regions at a distance

of 2 mm from complete section, at a rate of 2 μL/min by using a siliconized glass pipette stretched to 100 μM and filled with the cell suspension coupled to a 26G Hamilton syringe, mounted into the microinjector. A 1-minute pause between injections was observed before moving the syringe to allow cell deposition into the medullar tissue. The rats were premedicated with subcutaneous morphine (2.5 mg/kg) and Baytril (enrofloxacine, 5 mg/kg, Bayer, Germany) and anesthetized with 2% isoflurane in a continuous oxygen flow of 1 L/min. All animals were subjected to postsurgery cares, passive and active rehabilitation protocols as was previously described.[46,47] The animals were sacrificed after 8 weeks of evaluation. Histology: The animals were transcardially perfused with a 0.9% saline solution followed by 4% PFA in PBS, and 2 days incubation time in 30% sucrose before inclusion in Tissue-Teck OCT (Sakura Finetek U.S.A). Sagittal cryosections of 10 μm thickness were used for immunoassays. Every fifth section was collected for H&E staining to determine the anatomical structure and tissue volume calculations at the injured area. H&E-stained sections were scanned in a Pannoramic 250 Flash II scanner (3DHISTECH Ltd, Hungary) and images of approximately 20 mm^2 of medullar tissue (including the epicenter of the lesion) were acquired and with the Pannoramic viewer software. Immunohistochemistry. For assessment of differentiation, cryosectioned tissues (10 μm) were postfixed with 4% paraformaldehyde at room temperature for 10 minutes. After permeabilization with PBS containing 0.5% Triton and 2% goat serum (blocking solution), the primary antibodies were incubated overnight at 4°C. Cells or tissue sections were incubated with β-Tubulin III (α-mouse; Cat. MO15052 Neuromics) and Glial fibrillary acidic protein (GFAP) (α-rabbit; Cat. Z0334 DAKO) primary antibodies diluted 1:400 in blocking solution. After being rinsed three times with PBS, the cells were incubated with Oregon Green-Alexa488 and Alexa555 dye-conjugated secondary antibodies for 1 hour at room temperature. All cells were counterstained by incubation with DAPI for 5 minutes at room temperature followed by washing steps. Mounted sections were examined by both fluorescent microscopy (fluorescence microscope Leica DM6000B) and confocal microscopy (Confocal microscope Leica TCS-SP2-AOBS). The quantification of immunostaining was performed by using Image J software.

4.16 | Statistical analyses

Unpaired nonparametric *t* tests were used to evaluate statistical significance at $P \leq .05$. All quantitative and qualitative analyses are representative of at least n = 3 biological repeats for all experiments to give significant statistical power for reliability and validity of data.

ACKNOWLEDGMENTS

The authors acknowledge the support of the following people; Lauro Sumoy, High Content Genomics & Bioinformatics Unit. IGPT, Barcelona: Isabel Crespo Torres, for flow cytometry, IDIBAPS. Eric López Mocholi and Ana Alastrue Agudo for animal surgery and technical support. M.J.E. supported in part by the Program Ramon y Cajal (RYC-2010-06512), University of Barcelona Talent Retention program, FBG project 307900, MINECO project grant BFU2011-26596, BFU2014-54467-P and Fundació La Marató de TV3 2017/refs. 20172230, 20172231, and 20172110/FBG309768. V.M.M. lab was funded by FEDER/Ministerio de Ciencia e Innovación—Agencia Estatal de Investigación "RTI2018-095872-B-C21/ERDF," Fundació La Marató de TV3 2017/refs.20172230, 20172231, and 20172110, Agencia Valenciana de Innovación (AVI) INNVAL10/19/047, ACIF2019, and MINECO/FEDER, UE; Fondo Europeo de Desarrollo Regional (FEDER) incluido en el Programa Operativo FEDER de la Comunidad Valenciana 2014-2020). AV lab funded by Spanish Ministry of Science and Innovation grant SAF2014-55964-R (AV) co-funded by FEDER funds/European Regional Development Fund (ERDF)—a way to Build Europe, and the Catalan Government Agency AGAUR 2014-SGR-400(AV)." Research at MAB lab was funded by project SAF2013-45111-R of Societal Changes Programme of the Spanish Ministry of Economics and Competitiveness (MINECO) co-financed through the European Fund of Regional Development (FEDER), Fundación Botín and Banco Santander (Santander Universities Global Division) and Worldwide Cancer Research (WCR 16-1177). Dr Manel Esteller laboratory is supported by the EU Joint Programme—Neurodegenerative Disease Research (JPND); Cellex Foundation; the Health and Science Departments of the Catalan Government (Generalitat de Catalunya); the E-Rare (ERA-Net for research programs on rare diseases) and EuroRETT (a European network on Rett syndrome, funded by the European Commission under its sixth Framework Program since 2006).

CONFLICT OF INTEREST

The authors declared no potential conflicts of interest.

AUTHOR CONTRIBUTIONS

A.B.A.-P.: cell culture, RT-PCR, data analysis, manuscript preparation; J.R.: cell culture, RT-PCR, Western blot, data analysis, figure preparation, manuscript preparation; R.D.-M., S.M., M.E.: SNP/CNV array, isolation of DNA, data analysis, figure preparation, and bioinformatics; A.M.T.: assessment of telomeres, data analysis; M.J.O.: advice on clinical-grade cell culture, manuscript preparation; C.G.-B.: Rad51 and H2AX data collection, analysis, and figure preparation; C.B.: RT-PCR and analysis; A.V.: DNA damage, SirT1, apoptosis gene expression analysis, data analysis, manuscript preparation; I.S.-B.: DNA damage, SirT1, apoptosis gene expression analysis, data analysis; C.H.N., I.G.-M., F.V.P. for in depth SNP array analysis. V.M.-M.: rat spinal cord injury experiments, figure preparation; J.M.P.: gene expression data analysis, PCR methodology, primer design, figure design and preparation; M.A.B.: assessment of telomeres, funding; M.J.E.: original idea and overall project design, cell culture, data analysis, funding, wrote the manuscript, figures preparation, coordination of national and international teams.

DATA AVAILABILITY STATEMENT

The data that support the findings of this study are available on request from the corresponding author.

ORCID

Michael J. Edel https://orcid.org/0000-0002-5619-8680

REFERENCES

1. Miura K, Okada Y, Aoi T, et al. Variation in the safety of induced pluripotent stem cell lines. *Nat Biotechnol*. 2009;27:743-745.
2. Okita K, Ichisaka T, Yamanaka S. Generation of germline-competent induced pluripotent stem cells. *Nature*. 2007;448:313-317.
3. Takahashi K, Tanabe K, Ohnuki M, et al. Induction of pluripotent stem cells from adult human fibroblasts by defined factors. *Cell*. 2007;131:861-872.
4. Jin Z-B, Okamoto S, Xiang P, Takahashi M. Integration-free induced pluripotent stem cells derived from retinitis pigmentosa patient for disease modeling. *Stem Cells Translational Medicine*. 2012;1:503-509.
5. Mandai M, Kurimoto Y, Takahashi M. Autologous induced stem-cell-derived retinal cells for macular degeneration. *N Engl J Med*. 2017;377:792-793.
6. Edel MJ, Menchon C, Menendez S, Consiglio A, Raya A, Izpisua Belmonte JC. Rem2 GTPase maintains survival of human embryonic stem cells as well as enhancing reprogramming by regulating p53 and cyclin D1. *Genes Dev*. 2010;24:561-573.
7. Hanna J, Wernig M, Markoulaki S, et al. Treatment of sickle cell anemia mouse model with iPS cells generated from autologous skin. *Science*. 2007;318:1920-1923.
8. Woltjen K, Michael IP, Mohseni P, et al. piggyBac transposition reprograms fibroblasts to induced pluripotent stem cells. *Nature*. 2009;458:766-770.
9. Yu J, Vodyanik MA, Smuga-Otto K, et al. Induced pluripotent stem cell lines derived from human somatic cells. *Science*. 2007;318:1917-1920.
10. Fusaki N, Ban H, Nishiyama A, Saeki K, Hasegawa M. Efficient induction of transgene-free human pluripotent stem cells using a vector based on Sendai virus, an RNA virus that does not integrate into the host genome. *Proc Jpn Acad Ser B Phys Biol Sci*. 2009;85:348-362.
11. Stadtfeld M, Nagaya M, Utikal J, Weir G, Hochedlinger K. Induced pluripotent stem cells generated without viral integration. *Science*. 2008;322:945-949.
12. Warren L, Manos PD, Ahfeldt T, et al. Highly efficient reprogramming to pluripotency and directed differentiation of human cells with synthetic modified mRNA. *Cell Stem Cell*. 2010;7:618-630.
13. Warren L, Wang J. Feeder-free reprogramming of human fibroblasts with messenger RNA. *Curr Protoc Stem Cell Biol*. 2013;27:6.
14. Yoshioka N, Gros E, Li H-R, et al. Efficient generation of human iPSCs by a synthetic self-replicative RNA. *Cell Stem Cell*. 2013;13:246-254.
15. Zhou H, Wu S, Joo JY, et al. Generation of induced pluripotent stem cells using recombinant proteins. *Cell Stem Cell*. 2009;4:381-384.
16. Schlaeger TM, Daheron L, Brickler TR, et al. A comparison of non-integrating reprogramming methods. *Nat Biotechnol*. 2015;33:58-63.
17. Gore A, Li Z, Fung H-L, et al. Somatic coding mutations in human induced pluripotent stem cells. *Nature*. 2011;471:63-67.
18. Hussein SM, Batada NN, Vuoristo S, et al. Copy number variation and selection during reprogramming to pluripotency. *Nature*. 2011;471:58-62.
19. Ji J, Ng SH, Sharma V, et al. Elevated coding mutation rate during the reprogramming of human somatic cells into induced pluripotent stem cells. *Stem Cells*. 2012;30:435-440.
20. Koyanagi-Aoi M, Ohnuki M, Takahashi K, et al. Differentiation-defective phenotypes revealed by large-scale analyses of human pluripotent stem cells. *Proc Natl Acad Sci USA*. 2013;110:20569-20574.
21. Marión RM, Strati K, Li H, et al. A p53-mediated DNA damage response limits reprogramming to ensure iPS cell genomic integrity. *Nature*. 2009;460:1149-1153.
22. Nakagawa M, Koyanagi M, Tanabe K, et al. Generation of induced pluripotent stem cells without Myc from mouse and human fibroblasts. *Nat Biotechnol*. 2008;26:101-106.
23. Lopez-Serrano C, Torres-Espin A, Hernandez J, et al. Effects of the spinal cord injury environment on the differentiation capacity of human neural stem cells derived from induced pluripotent stem cells. *Cell Transplant*. 2016;25:1833-1852.
24. Bienvenu F, Jirawatnotai S, Elias JE, et al. Transcriptional role of cyclin D1 in development revealed by a genetic-proteomic screen. *Nature*. 2010;463:374-378.
25. Casimiro MC, Crosariol M, Loro E, et al. ChIP sequencing of cyclin D1 reveals a transcriptional role in chromosomal instability in mice. *J Clin Invest*. 2012;122:833-843.
26. Smith K, Dalton S. Myc transcription factors: key regulators behind establishment and maintenance of pluripotency. *Regen Med*. 2010;5:947-959.
27. Walz S, Lorenzin F, Morton J, et al. Activation and repression by oncogenic MYC shape tumour-specific gene expression profiles. *Nature*. 2014;511:483-487.
28. Feng B, Jiang J, Kraus P, et al. Reprogramming of fibroblasts into induced pluripotent stem cells with orphan nuclear receptor Esrrb. *Nat Cell Biol*. 2009;11:197-203.
29. Aasen T, Raya A, Barrero MJ, et al. Efficient and rapid generation of induced pluripotent stem cells from human keratinocytes. *Nat Biotechnol*. 2008;26:1276-1284.
30. Raya A, Rodríguez-Pizà I, Guenechea G, et al. Disease-corrected haematopoietic progenitors from Fanconi anaemia induced pluripotent stem cells. *Nature*. 2009;460:53-59.
31. Chalermrujinanant C, Michowski W, Sittithumcharee G, Esashi F, Jirawatnotai S. Cyclin D1 promotes BRCA2-Rad51 interaction by restricting cyclin A/B-dependent BRCA2 phosphorylation. *Oncogene*. 2016;35:2815-2823.
32. Hydbring P, Malumbres M, Sicinski P. Non-canonical functions of cell cycle cyclins and cyclin-dependent kinases. *Nat Rev Mol Cell Biol*. 2016;17:280-292.
33. Jirawatnotai S, Sittithumcharee G. Paradoxical roles of cyclin D1 in DNA stability. *DNA Repair (Amst)*. 2016;42:56-62.
34. Jirawatnotai S, Hu Y, Michowski W, et al. A function for cyclin D1 in DNA repair uncovered by protein interactome analyses in human cancers. *Nature*. 2011;474:230-234.
35. Ambrosio S, Amente S, Napolitano G, Di Palo G, Lania L, Majello B. MYC impairs resolution of site-specific DNA double-strand breaks repair. *Mutat Res*. 2015;774:6-13.
36. Ganesan S. MYC, PARP1, and chemoresistance: BIN there, done that? *Sci Signal*. 2011;4:pe15.
37. Muvarak N, Kelley S, Robert C, et al. c-MYC generates repair errors via increased transcription of alternative-NHEJ factors, LIG3 and PARP1, in tyrosine kinase-activated Leukemias. *Mol Cancer Res*. 2015;13:699-712.
38. S. Pyndiah, S. Tanida, K. M. Ahmed, E. K. Cassimere, C. Choe, D. Sakamuro, c-MYC suppresses BIN1 to release poly(ADP-ribose) polymerase 1: a mechanism by which cancer cells acquire cisplatin resistance, *Sci Signal* 4, ra19 (2011).
39. Li G, Ruan X, Auerbach RK, et al. Extensive promoter-centered chromatin interactions provide a topological basis for transcription regulation. *Cell*. 2012;148:84-98.
40. Martinez P, Thanasoula M, Muñoz P, et al. Increased telomere fragility and fusions resulting from TRF1 deficiency lead to degenerative pathologies and increased cancer in mice. *Genes Dev*. 2009;23:2060-2075.
41. Masson JY, Tarsounas MC, Stasiak AZ, et al. Identification and purification of two distinct complexes containing the five RAD51 paralogs. *Genes Dev*. 2001;15:3296-3307.
42. Plo I, Laulier C, Gauthier L, Lebrun F, Calvo F, Lopez BS. AKT1 inhibits homologous recombination by inducing cytoplasmic retention of BRCA1 and RAD51. *Cancer Res*. 2008;68:9404-9412.
43. Takata M, Sasaki MS, Tachiiri S, et al. Chromosome instability and defective recombinational repair in knockout mutants of the five Rad51 paralogs. *Mol Cell Biol*. 2001;21:2858-2866.
44. Kostyrko K, Mermod N. Assays for DNA double-strand break repair by microhomology-based end-joining repair mechanisms. *Nucleic Acids Res*. 2016;44:e56.

45. De Bonis ML, Ortega S, Blasco MA. SIRT1 is necessary for proficient telomere elongation and genomic stability of induced pluripotent stem cells. *Stem Cell Rep*. 2014;2:690-706.
46. Kobayashi Y, Okada Y, Itakura G, et al. Pre-evaluated safe human iPSC-derived neural stem cells promote functional recovery after spinal cord injury in common marmoset without tumorigenicity. *PLoS One*. 2012;7:e52787.
47. Rosenzweig ES, Brock JH, Lu P, et al. Restorative effects of human neural stem cell grafts on the primate spinal cord. *Nat Med*. 2018;24:484-490.
48. Lee YL, Peng Q, Fong SW, et al. Sirtuin 1 facilitates generation of induced pluripotent stem cells from mouse embryonic fibroblasts through the miR-34a and p53 pathways. *PLoS One*. 2012;7:e45633.
49. Smyth GK. Linear models and empirical Bayes methods for assessing differential expression in microarray experiments. *Stat Appl Genet Mol Biol*. 2004;3: Article 3.
50. Subramanian A, Tamayo P, Mootha VK, et al. Gene set enrichment analysis: a knowledge-based approach for interpreting genome-wide expression profiles. *Proc Natl Acad Sci USA*. 2005;102(43):15545-15550.
51. Ben-Porath I, Thomson MW, Carey VJ, et al. An embryonic stem cell-like gene expression signature in poorly differentiated aggressive human tumors. *Nat Genet*. 2008;40:499-507.

SUPPORTING INFORMATION

Additional supporting information may be found online in the Supporting Information section at the end of this article.

How to cite this article: Alvarez-Palomo AB, Requena-Osete J, Delgado-Morales R, et al. A synthetic mRNA cell reprogramming method using *CYCLIN D1* promotes DNA repair, generating improved genetically stable human induced pluripotent stem cells. *Stem Cells*. 2021;39:866–881. https://doi.org/10.1002/stem.3358